ACS OMEGA

http://pubs.acs.org/journal/acsodf

Article

Study on the Fluidization Quality Characterization Method and Process Intensification of Fine Coal Separation in a Vibrated Dense Medium Fluidized Bed

Enhui Zhou,* Yadong Shan, Linhai Li, Fanshun Shen, Enkhsaruul Byambajav, Bo Zhang, and Changxing Shi

Cite This: *ACS Omega* 2021, 6, 14268−14277

Read Online

ACCESS | Metrics & More | Article Recommendations

ABSTRACT: Uniform and stable bed density is the basis of efficient coal separation by a gas−solid dense medium fluidized bed. The traditional air dense medium fluidized bed (ADMFB) is a kind of bubbling bed. By introducing vibration energy, a vibrated dense medium fluidized bed (VDMFB) with uniform and stable bed density can be formed, where the bubble merger is suppressed, the gas−solid contact can is strengthened, and the fluidization quality is also improved. In this paper, the transfer process of vibration energy in a fluidized bed is studied in detail. By calculating the coherence of pressure signals induced by vibration energy and bubbles at different bed heights, the suppression effect of vibration energy on bubble merger is analyzed. The coefficient R_{imp} to quantitatively evaluate the improvement effect of vibration energy on the fluidization quality is proposed. The differences and incentives of density uniformity and stability in different height bed areas have been clarified under different vibration parameters and gas flow parameters. It is proposed that the optimal separation bed height area of VDMFB is about H = 40−150 mm. The separation effect of the ADMFB and the VDMFB on 1−6 mm fine coal was compared. The results show that, compared with the ADMFB, the VDMFB reduces the separation probable error, E, from 0.134 to 0.083 g/cm^3, and the ash content of the clean coal is reduced from 18.83 to 14.97%. The vibration energy significantly improves the fluidization quality of the ADMFB and the separation effect of fine coal.

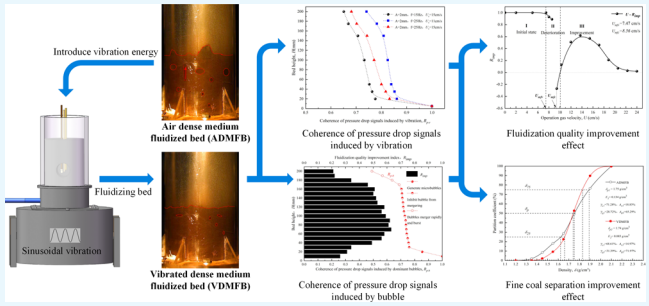

1. INTRODUCTION

Coal is one of the most important fossil energy sources in the world. The world's annual coal production exceeds 8 billion tons.[1] Coal is the basis for alleviating the global energy shortage and ensuring energy security. Affected by the original plant species and accumulation environment, crustal movement, and deposition time, the composition and properties of coal are complex and diverse, containing many impurities. Direct application of coal without separating and impurity removal will cause serious environmental pollution.[2] In China, more than two-thirds of coal is distributed in arid and water shortage areas. Fluidization dry separation technology is an effective way to solve the problem of coal separation in arid and water shortage areas. The dry separation technologies with coarse coal (+6 mm) such as air jigging,[3] air table,[4] vibrating inclined deck,[5] FGX dry separator,[6] and air dense medium fluidized bed (ADMFB)[7] are mature. However, there is no significant breakthrough in dry separation research of fine coal (−6 mm). With the popularization of fully mechanized coal mining technology, the content of −6 mm fine coal in raw coal is increasing. The demand for efficient dry separation of fine coal is more and more urgent. A lot of research[8−10] has shown that a vibrating dense medium fluidized bed (VDMFB) can be formed by applying vibration energy to an ADMFB, which can strengthen the gas−solid contact and form a micro-bubble fluidization environment with uniform and stable density suitable for fine coal separation. Therefore, the VDMFB provides an effective way for dry clean separation of fine coal.

VDMFB is a typical gas−solid two-phase flow system, and the motion between the gas-phase and solid-phase is complex. The uniformity and stability of the bed are the basis of efficient separation of materials in a gas−solid dense medium fluidized bed. In the fluidized bed dominated by Geldart B particles, bubbling fluidization will occur once the gas velocity exceeds the minimum fluidization velocity. At this stage, the formation and movement of bubbles lead to low gas−solid contact and uneven

Received: February 25, 2021
Accepted: May 13, 2021
Published: May 25, 2021

Table 1. Research Results on the Evaluation Method of Mixing and Uniformity of Bed Density

researcher	evaluation method
Mores[11]	the bed density uniformity is evaluated by the fluctuation characteristics of the bed porosity signal. It is considered that the fluidization is uniform if the fluctuation amplitude of the porosity signal is large and the frequency is low, otherwise, the fluidization is not uniform.
Mujumdar[12]	the bed uniformity was judged according to the average deviation of bed porosity. It is proposed that the critical value of bed uniformity and non-uniformity is vibration intensity, $A\omega^2/g$. When $A\omega^2/g < 4$, the bed density is uniform.
Btatu[13]	the volume fraction of the emulsified phase (V_e) under the vibration condition and that under the non-vibration condition were compared under a heat transfer test. The higher the volume fraction of the emulsion phase under the vibration condition, the more uniform the bed density is. The results show that the volume ratio of the emulsion phase under the vibration condition and non-vibration condition is 1.95.
Gutman[14]	the bed uniformity was evaluated by the deviation between bed porosity and average value, and the minimum value was $5\%.\mathrm{l}(\varepsilon_i - \bar{\varepsilon})/\bar{\varepsilon} \times 100\%\mathrm{l}_{min} = 5\%$
Jin[15]	based on the vibration intensity K, the kirpichev number K_i of particles, gas velocity ratio U/U_{mf}, bed height H_0, and vibration amplitude A, the evaluation correlations are obtained, $C_v = \left(\frac{K_i}{K}\right)^{0.5} \frac{U}{U_{mf}} \left(\frac{H_0}{A}\right)^{0.4}$, when $6 \le C_v \le 18$, the bed uniformity is better.
Tanaka[16]	the conditions of uniform particle mixing and bed density are as follows:$1 - \varepsilon_{mf} < \frac{\rho_2}{\rho_1} < \frac{1}{1-\varepsilon_{mf}}$ and $0.5 < \frac{d_p}{D_1}\left(\frac{\rho_2}{\rho_1}\right)^2 < 2$
Di Maio[17]	by comparing the forces of different particles, the discriminant of uniform mixing is obtained $s \le \frac{(1-\varepsilon)(1-d')(1-\delta)+d'}{\delta(d'+\varepsilon-\varepsilon d')+(1-\delta)}$
Lv[18]	according to the experimental fitting, the transverse diffusion coefficient of fine coal particles in the fluidized bed is obtained $D_x = 3.32393 \times 10^{-5} + \frac{1.02424 \times 10^{-8} \times (e^{0.86977u} - 1)}{0.86977}$, the bed density uniformity is qualitatively judged according to the transverse diffusion coefficient.

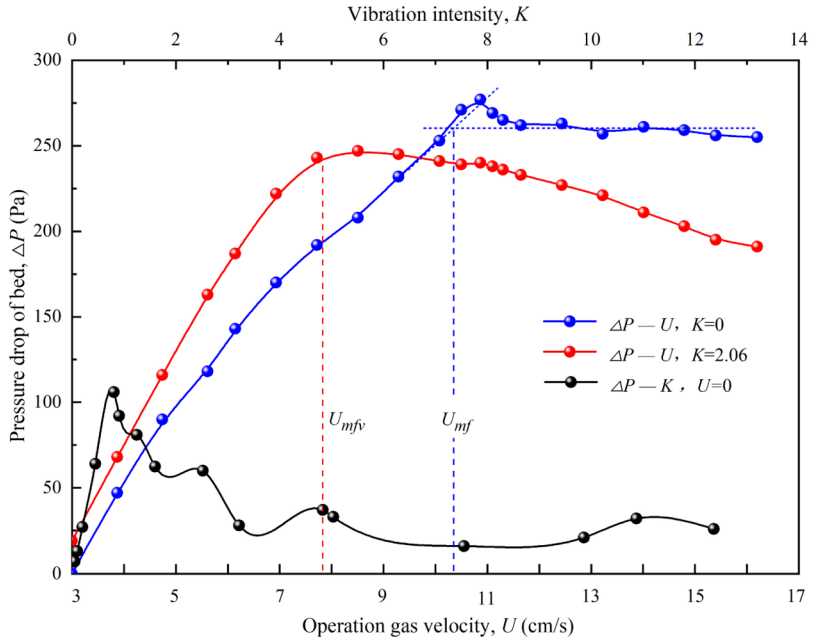

Figure 1. Fluidization curves under different vibrations and operation gas velocities.

distribution of bed density along the radial and axial directions, which is not suitable for fine coal separation. Based on its experimental conditions and application background, different scholars put forward different methods to evaluate the uniform stability of bed density, as shown in Table 1.

Mores, Mushtaev, and Gutman judged the bed uniformity according to the average deviation of voidage. Mores and Gutman qualitatively judged the uniformity of the bed density mainly according to the change law of the bed voidage signal. Mushtaev et al. proposed that the critical value of bed uniformity and non-uniformity was the vibration intensity $K = 4$, which avoided the influence of gas velocity. Btatu et al. determined the uniformity of a particle bed according to the gas flow of the emulsion phase, so the measurement accuracy of the test was difficult to control. For the vibrated fluidized bed for material separation, the bed uniformity is usually evaluated by the spatial distribution variance of bed density, and the bed stability is evaluated by the temporal distribution variance of bed density. Jin H defined the discrimination coefficient of uniformity based on vibration intensity, particle properties, and bed height and determined the range of operation parameters to realize the uniformity and stability of the particle bed. However, the kirpitchev number of different particles is completely different, and it is difficult to measure in time. From the perspective of studying the mixing behavior of different particles, Tanaka, Francesco P. Di Maio, and Lv B proposed a discriminant respectively for different particle mixing degrees based on basic physical parameters such as particle size, density, and force. Furthermore, after grasping the degree of particle mixing, the bed density uniformity was evaluated. In general, the scholars have analyzed the improvement effect of vibration energy on fluidization quality of the air fluidized bed from the perspective of fluidization uniformity and stability. Many of the existing research results are only applicable to the operating conditions

https://doi.org/10.1021/acsomega.1c01034
ACS Omega 2021, 6, 14268−14277

set by researchers, and the basic parameters such as particle size and density cannot be collected in real time. Therefore, it is not suitable to apply these methods to judge the uniformity of the bed density of a VDMFB, which is used to create a uniform fluidized bed suitable for coal separation by density.

Based on the previous statistical analysis and research on the uniformity and stability of vibrated fluidized bed, this paper focuses on the quantitative evaluation method of the improvement degree of fluidization quality, analyzes the improvement process and mechanism, and explores the best separation area and fine coal separation effect.

2. RESULTS AND DISCUSSION

2.1. Characterization Method of the Effect of Vibration on Fluidization Quality. The whole power of fluidization in a VDMFB comes from the vibration energy and gas flow. The single action and interaction of vibration and flow can lead to different fluidization behaviors. Figure 1 shows the fluidization characteristic curves of an ordinary gas−solid fluidized bed ($K = 0$, $U > 0$), an ordinary vibrated bed ($K > 0$, $U = 0$), and a VDMFB ($K > 0$, $U > 0$). The bed height difference corresponding to pressure drop is 15 mm.

In the ordinary vibrated bed ($K > 0$, $U = 0$), the vibration led to dense accumulation of particles, and the pressure drop of the bed increased gradually when $K = 0-1$. The bed pressure drop decreased gradually until irregular fluctuation at a small level when $K > 1$, which indicated that the particles vibrated randomly driven by the vibration energy through the inelastic collision, and the particles' motion was disordered. After the introduction of gas flow, the pressure drop of ordinary vibrated bed ($K > 0$, $U = 0$) and the VDMFB ($K > 0$, $U > 0$) increased linearly with the increase of operating gas velocity and the fluidization changed from the fixed bed to the fluidized state. The difference is that there is a turning point in the pressure drop curve of the ordinary gas−solid fluidized bed, while there is no obvious turning point in the pressure drop curve of the VDMFB from the fixed bed to the fluidized state. In addition, the initial fluidization gas velocity U_{mfv} of the VDMFB is lower than that of the ordinary gas−solid fluidized bed. Before fluidization, the pressure drop ΔP_b of the VDMFB was higher than that of the ordinary gas−solid fluidized bed, but the relationship was reversed after fluidization. The relative motion between particles was strengthened with the introduction of vibration, the gas between particles was squeezed, and the particle gap was reduced, resulting in a higher pressure drop in the VDMFB. With the increase of gas velocity, the gap between the particles increased. The oscillation displacement of the particles increased driven by the vibration energy, which promoted the loosening of particles. Therefore, $U_{mfv} < U_{mf}$ and the VDMFB completely fluidized when the operating gas velocity exceeded U_{mfv}.

When $A = 2$ mm, $f = 25$ Hz, the bed density variance under different gas velocities was measured, and the improvement index of vibration energy on fluidization quality (R_{imp}) was calculated, as shown in Figure 2. In the fixed bed state ($U < 7.47$ cm/s), the bed density uniformity index (I_u) is equal to 1, and the bed density is stable. With the increase of gas velocity, the VDMFB fluidized first. When $7.47 < U < 9.43$ cm/s, $I_{u,v}$ decreasing gradually, the ordinary gas−solid fluidized bed (ADMFB) has not been fluidized, and the fluidization quality of the two kinds of fluidized beds cannot be compared. Therefore, only $I_{u,v}$ was used to characterize the fluidization quality change of the VDMFB. $I_{u,v} < 1$, and it meant that the introduction of vibration led to the decrease of bed density uniformity and stability. When $9.43 < U < 10.11$ cm/s, the initial fluidization gas velocity of the ADMFB is lower than that of the VDMFB. Therefore, when $U = 9.43-10.11$ cm/s, the VDMFB has been completely fluidized, there are more bubbles in the bed, and the dense medium particles migrate directionally. On the other hand, the ADMFB has just begun to fluidize, and there are fewer bubbles. Therefore, at this stage, the bed density fluctuation of the ADMFB is smaller, $I_{u,v} < I_{u,c}$, and the R_{imp} value is negative. Therefore, in the range of 7.47−10.11 cm/s, the vibration energy actually worsened the fluidized quality. With the further increase of gas velocity, more and more bubbles were produced in the VDMFB, and the fluctuation of bed density was intensified. At this time, the inhibition effect of vibration energy on bubbles was gradually shown, and R_{imp} increased, which indicated that the bed density of the VDMFB remained relatively stable. When the gas velocity was too high, the transfer effect of vibration energy in the bed was weakened, and the uniformity of the particle bed was deteriorating. R_{imp} gradually tended to zero, and the improvement effect of vibration on the bed density uniformity almost disappears.

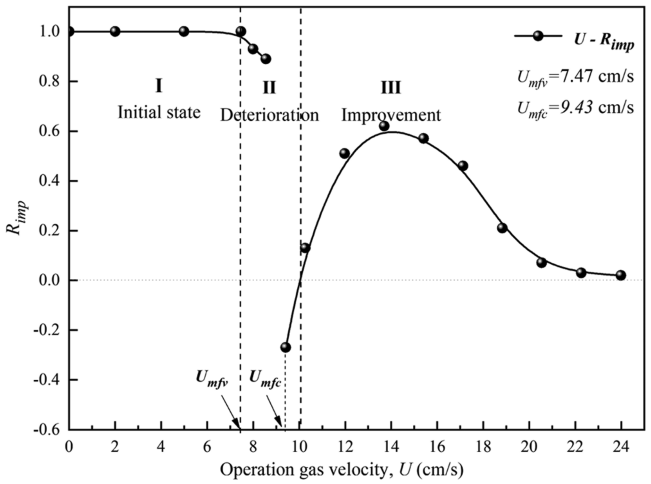

Figure 2. Fluidization quality improvement effect of the VDMFB under different operation gas velocities.

2.2. Improvement Mechanism of Vibration Energy on Fluidization Quality. The periodic motion of the distributor and the wall transferred the vibration energy to the particles. The friction between particles was overcome, and the kinetic energy of particles was enhanced. The operating gas velocity was set to 11 cm/s, and the bed densities at the height of 25, 50, 75, 100, 125, 150, and 175 mm were measured. Then, the corresponding bed density fluctuation standard deviation was calculated to explore the influence of amplitude and vibration frequency on the uniformity and stability of bed density distribution. The results are shown in Figure 3.

The variation trends and amplitudes of the $\sigma_\rho-f$ curve and $\sigma_\rho-A$ curve were similar, and the bed density fluctuation was similar to the condition of low-amplitude and low-frequency. When $f = 26.3$ Hz and $A = 2.21$ mm, the curves of $\sigma_\rho-f$ and $\sigma_\rho-A$ reach the lowest points respectively, and the vibration parameters of the two conditions are similar. With the further increase of vibration frequency and amplitude, the $\sigma_\rho-f$ curve increases rapidly, while the $\sigma_\rho-A$ curve increases slowly and tends to be stable. When the vibration frequency was too high, the kinetic energy of particles was too large, and the density distribution of the bed was not uniform. With the increase of the amplitude, the transfer efficiency of vibration energy in the bed

https://doi.org/10.1021/acsomega.1c01034
ACS Omega 2021, 6, 14268−14277

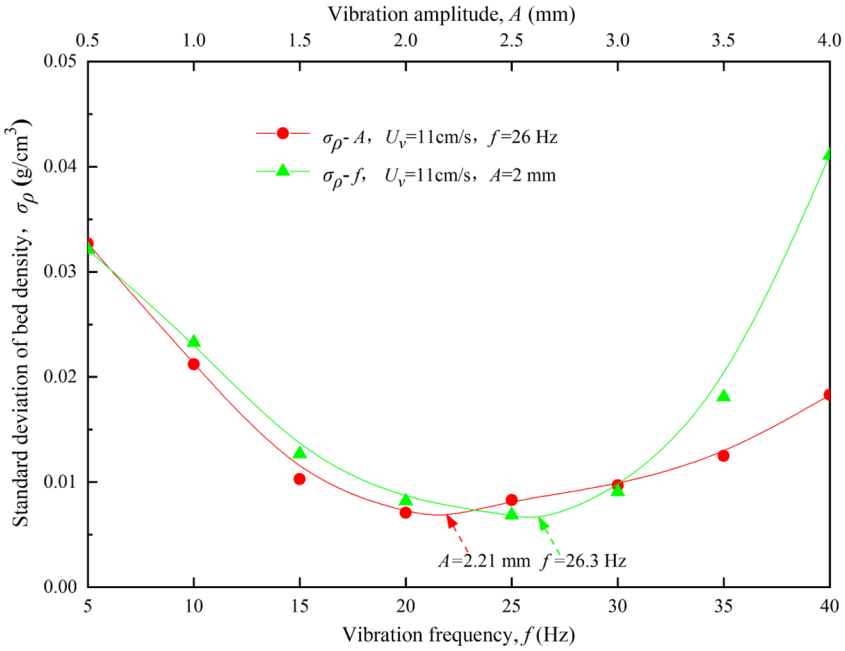

Figure 3. Standard deviation of bed density for different vibration amplitudes and frequencies.

gradually decreased, which limited the movement activity of the heavy particles. In the range of this experiment, the bed density will not undulate with the increase of amplitude.

Furthermore, the pressure signals with the same frequency as the vibration table were extracted from the pressure signals at different heights, and the coherence analysis was carried out with the pressure signals at the bed height of 5 mm. The results are shown in Figure 4.

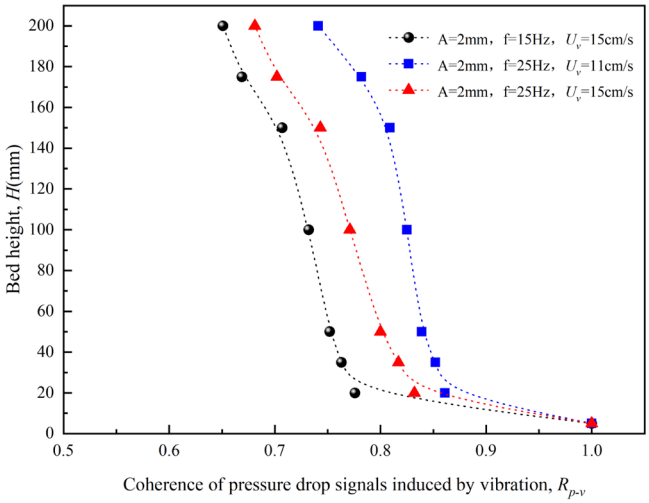

Figure 4. Coherence of pressure drop signals induced by vibration.

It is shown in Figure 4 that the variation law of pressure signal coherence ($R_{p\text{-}v}$) caused by vibration is similar, and the difference lies in the strength of coherence under the three kinds of vibration and gas flow parameters. In the region of $H \approx 5-40$ mm, $R_{p\text{-}v}$ decreases rapidly. This is because this area is close to the gas distributor, and it is the main generation area of random microbubbles. The microbubbles caused significant random disturbance to the periodic pressure fluctuation, and the inhibition effect of vibration energy was difficult to fully break the microbubbles. In the region of $H \approx 40-150$ mm, $R_{p\text{-}v}$ continues to decrease, and the decrease is very low. It shows that the bubble can be restrained and the gas−solid contact can be strengthened. A uniform and stable continuous bed was formed, which is suitable for the uniform transmission and dissipation of vibration energy and the separation of fine coal. In the region of $H > 150$ mm, the decrease of $R_{p\text{-}v}$ increases, but it is lower than that in the region of $H \approx 5-40$ mm. This result showed that the speed of bubble coalescence was faster in the top area of the bed, and the bubble size and velocity increased rapidly. At the same time, the uneven dissipation of vibration energy was accelerated, and the coherence of pressure signal induced by vibration was also reduced. The effect of vibration energy to particles and bubbles in the upper region was weak, and the fluidization of upper particle bed was closer to that of the ordinary gas−solid fluidized bed.

Comparing the operating conditions, it can be found that the decrease of $R_{p\text{-}v}$ is always significant with the condition of $A = 2$ mm, $f = 15$ Hz, $U_v = 15$ cm/s. It is indicated that the vibration energy cannot effectively inhibit the bubble evolution, resulting in irregular dissipation of vibration energy and disordered movement of particles, which is not conducive to the separation of fine coal. When $A = 2$ mm, $f = 25$ Hz, $U_v = 11$ cm/s, the decrease of $R_{p\text{-}v}$ is the lowest. The result shows that the vibration energy transfer efficiency is quite high under the vibration condition, and the vibration energy has a significant effect on inhibiting bubble evolution, forming a stable fluidization environment suitable for fine coal separation.

2.3. Improvement Effect of Vibration Energy on Fluidization Quality. In the case of no vibration, such as the ADMFB, the coherence of pressure drop signals caused by bubbles at different bed heights gradually decreases (Figure 5). The results show that bubbles are rapidly generated from the bottom of the bed ($H < 40$ mm) and merge at a relatively uniform speed in the upper and middle parts of the bed ($H > 40$ mm), resulting in channel flow, dead zone, and particle back-mixing. The bed pressure drop fluctuates sharply and the density distribution is uneven. After the introduction of vibration, the

https://doi.org/10.1021/acsomega.1c01034
ACS Omega 2021, 6, 14268−14277

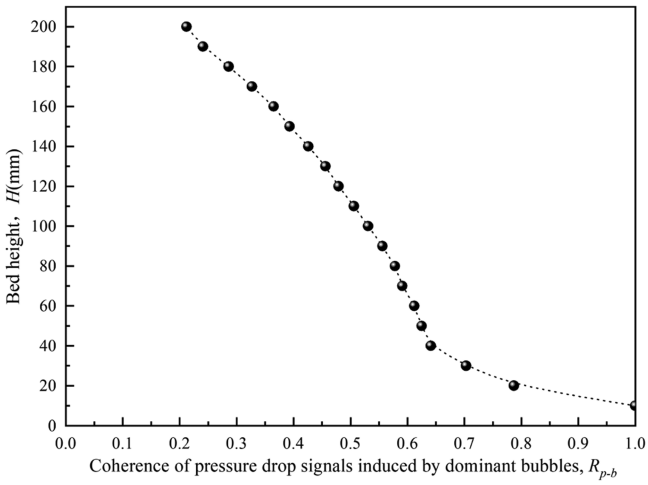

Figure 5. Coherence of pressure drop signals induced by dominant bubbles without vibration.

activity of particles increases and the bubble coalescence strength is suppressed.

Previous studies[19] show that the dominant frequency of pressure fluctuation caused by dominant bubbles is 4.5−7.5 Hz. To determine the suppression effect of vibration energy on bubbles, the coherence $R_{p\text{-}b}$ and R_{imp} between the pressure signals at different bed heights with the frequency of 6 Hz and the pressure signal at 5 mm were calculated, as shown in Figure 6−8.

The result shows that the bubble merging strength has a negative correlation with the improvement effect of vibration energy on fluidization quality. According to the variation rule of $R_{p\text{-}b}$ along with the bed height, the bed can be divided into three regions, that is, microbubble formation region (H < 40 mm), bubble merging inhibition region (H = 40−150 mm), and bubble fast merging and breaking region (H > 150 mm). In the microbubble formation region (H < 40 mm), the impact of the periodically moving distributor and the dense medium particles frequently sheared the gas flow, and many microbubbles were generated, which made $R_{p\text{-}b}$ decrease rapidly. The microbubbles generated randomly caused significant random disturbance to the bed density, which limited the improvement effect of vibration energy on fluidization quality. Therefore, the R_{imp} values in the area (H < 40 mm) are almost the same as the operating conditions shown in Figures 6−8. In the bubble merging inhibition region (H = 40−150 mm), the merging of the bubble competed with the restraining effect of vibration energy. When A = 2 mm, f = 15 Hz, and U_v = 15 cm/s (Figure 6), the gas velocity was larger, and the vibration intensity was weaker, and the $R_{p\text{-}b}$ value continued to decrease. Although the R_{imp} value increases (H = 40−70 mm), it immediately decreases (H = 70−150 mm), indicating that the coalescence of bubbles was not suppressed, and the bubbles caused an obvious bed density disturbance. When A = 2 mm, f = 25 Hz, and U_v = 15 cm/s (Figure 8), the vibration intensity increases with the constant gas velocity and the decrease of pressure coherence $R_{p\text{-}b}$ caused by bubbles decreases. The results show that the vibration can enhance the inhibition effect on bubble coalescence, reduce the bubble coalescence speed, and the R_{imp} value is close to 0.5 in a wide range of bed (H = 40−140 mm). When A = 2 mm, f = 25 Hz, and U_v = 11 cm/s (Figure 7) the gas velocity decreases with the constant vibration intensity, and the pressure coherency $R_{p\text{-}b}$ caused by the bubbles in the region (H = 40−160 mm) further decreases, which is stable at about 0.7 and R_{imp} value is stable at about 0.5. It meant that the bubble size was stable in this region, and the vibration energy can effectively suppress the bubble evolution in a wider region of the particle bed. In the bubble fast merging and breaking region (H > 150 mm), $R_{p\text{-}b}$ and R_{imp} values decreased rapidly. It showed that the vibration energy in this region dissipated rapidly, and the restraint of vibration on the behavior of particles and bubbles was greatly weakened. A large number of rapidly rising bubbles broke away from the suppression of vibration energy and merged rapidly in this region, which worsened the fluidization quality. Comparing with Figures 6−8, it can be found that the vibration energy has the

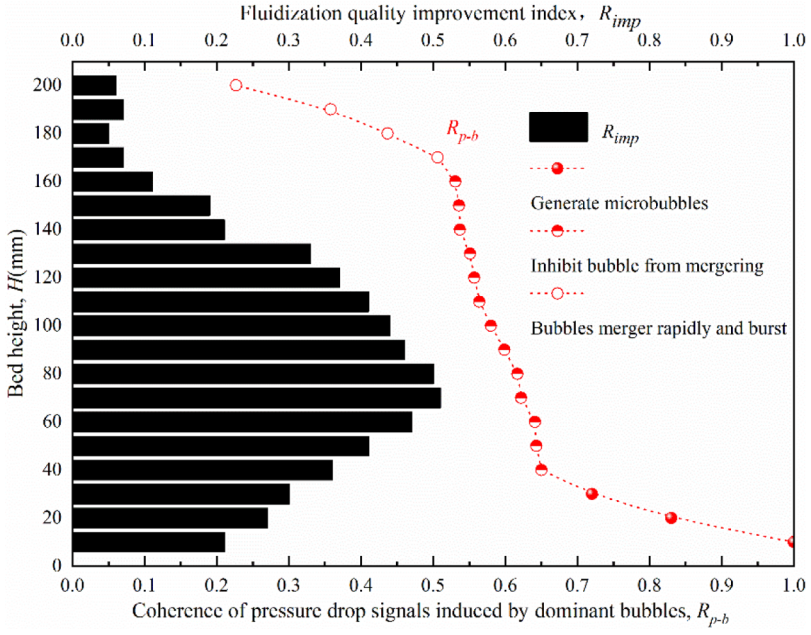

Figure 6. Coherence of pressure drop signals induced by dominant bubbles for A = 2 mm, f = 15 Hz, U_v = 15 cm/s.

https://doi.org/10.1021/acsomega.1c01034
ACS Omega 2021, 6, 14268−14277

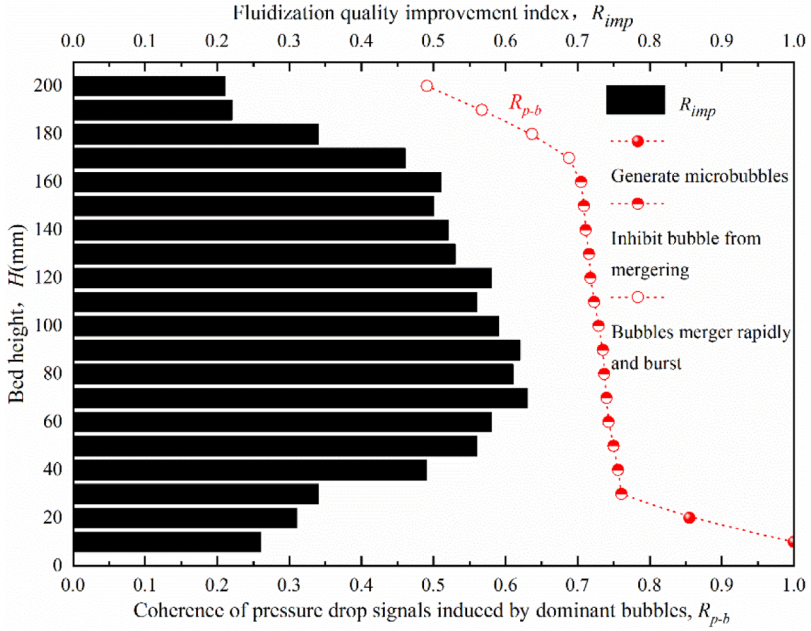

Figure 7. Coherence of pressure drop signals induced by dominant bubbles for A = 2 mm, f = 25 Hz, U_v = 11 cm/s.

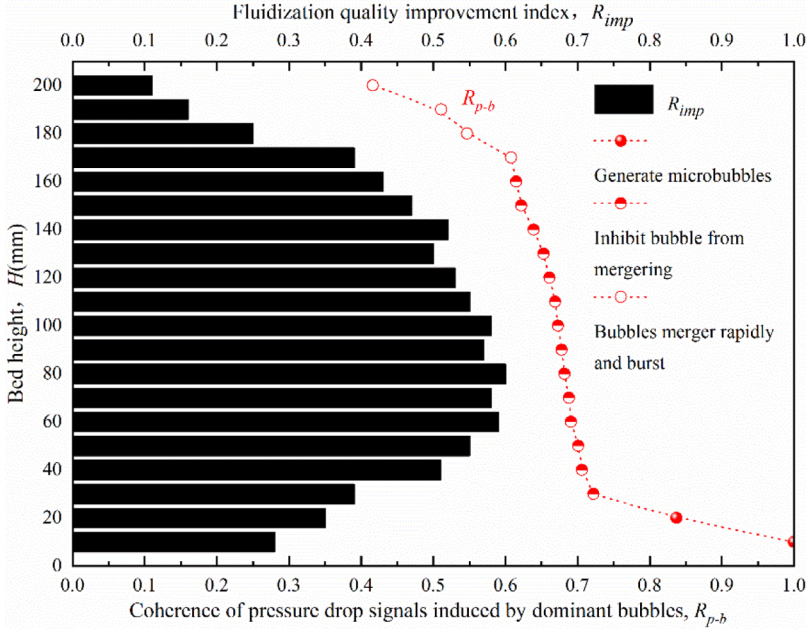

Figure 8. Coherence of pressure drop signals induced by dominant bubbles for A = 2 mm, f = 25 Hz, U_v = 15 cm/s.

best effect on improvement of fluidization quality with the condition of A = 2 mm, f = 25 Hz, and U_v = 15 cm/s.

2.4. Optimum Separation Area and Separation Effect of Fine Coal. Furthermore, the density standard deviation and skewness distribution along the height were compared under conditions of vibration (A = 2 mm, f = 25 Hz) and no vibration (A = 0, f = 0) to explore the effect of vibration on the uniform stability of the ADMFB. As shown in Figure 9a, the standard deviation σ_ρ of the bed density of the VDMFB (0.0047−0.0329 g/cm^3) is significantly lower than that of the ADMFB (0.0366−0.0976 g/cm^3). In the ADMFB, the standard deviation σ_ρ of bed density increases gradually along the bed height, which is the inevitable result of bubble coalescence and growth. According to the coherence results of pressure signal caused by vibration energy and bubbles in Sections 3.2 and 3.3, the distribution of σ_ρ is the result of vibration energy effectively restraining bubble evolution. Compared with the ADMFB, the bed density standard deviation of VDMFB decreased by 81.49%.

As shown in Figure 9b, the bed density skewness SK_ρ of the ADMFB increases gradually with the increase of bed height, whereas SK_ρ of the VDMFB has three stages, that is, gradually decreasing → basically stable → gradually increasing. In the bottom region (H < 40 mm), the SK_ρ of the ADMFB is less than 0, which indicated that the density in most areas was greater than the average density, and the density in a few areas was smaller due to the existence of discrete bubbles. In the VDMFB, the vibration energy broke the discrete bubbles into microbubbles and diffuses evenly, which made the density in most areas lower

https://doi.org/10.1021/acsomega.1c01034
ACS Omega 2021, 6, 14268−14277

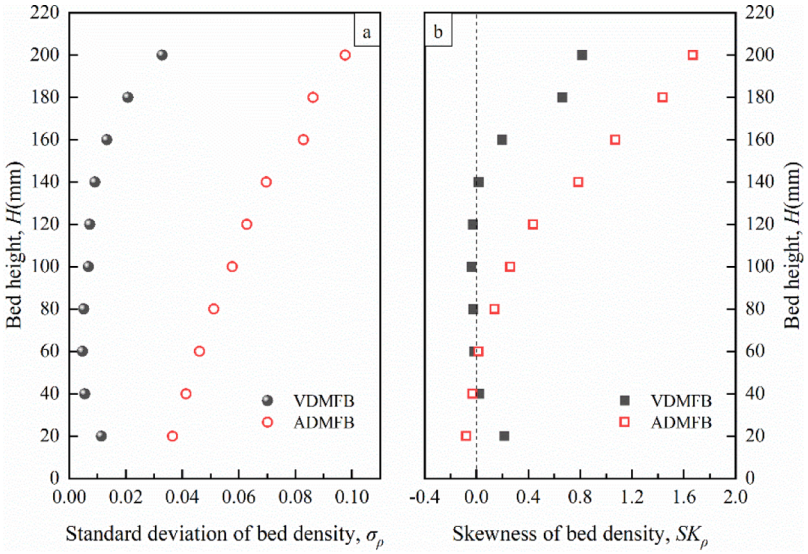

Figure 9. Comparison of standard deviation (a) and skewness (b) of bed density between the ADMFB and the VDMFB.

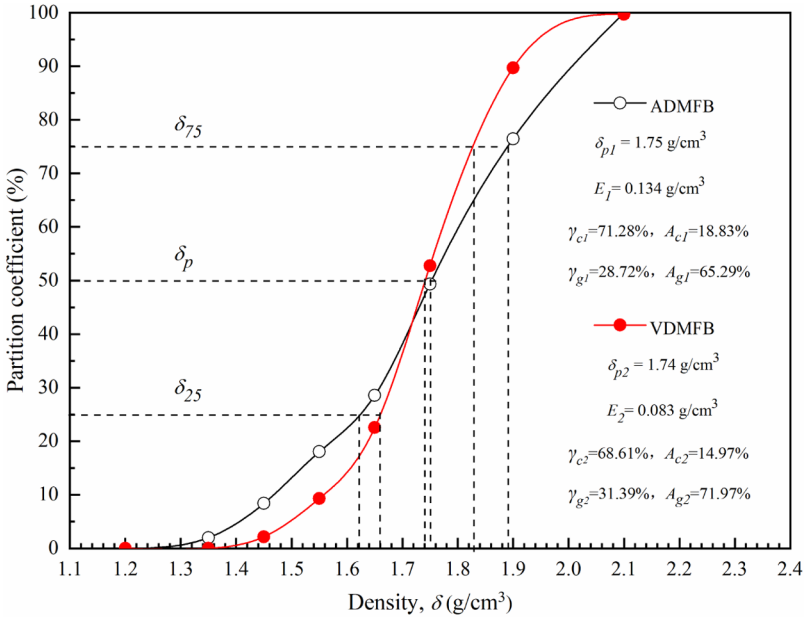

Figure 10. Partition curve of 1−6 mm fine coal separated by the ADMFB and VDMFB.

than the average density, and the dead zone density in the local areas due to short circuit of gas flow is larger. Therefore, SK_ρ of the VDMFB is more than 0. In the middle and upper regions (H > 140 mm), SK_ρ of the ADMFB is more than 0 and increases gradually. Combined with the increasing trend of σ_ρ in this area in Figure 9a, it indicated that there were many large bubbles in the region (H > 40 mm), forming a regional dilute phase bed dominated by bubbles, resulting in the density in most areas being lower than the average density, and the stability of the bed density was poor. In the VDMFB, SK_ρ of the middle region (H = 40−140 mm) is about 0, and it is basically stable. It indicated that the bed density fluctuation in the middle region was in a narrow range. The bed density distribution was more uniform, which was suitable for the separation of fine coal. In the upper region (H > 140 mm), SK_ρ of the VDMFB is more than 0 and increases gradually. The reason is that the efficiency of vibration energy transfer is reduced, the small bubbles merge into large bubbles quickly, forming a dilute phase bed around the bubbles and deteriorating the fluidization quality. In general, the VDMFB can effectively improve the fluidization quality of the bed, strengthen the uniformity and stability of the bed density distribution, and create a fluidization environment for the effective separation of fine coal.

Three kilograms of fine coal with a size of 1−6 mm was fed into the ADMFB (U_v = 11 cm/s) and VDMFB (A = 2 mm, f = 25 Hz, U_v = 11 cm/s) respectively for the separation test. Clean coal and tailing coal were taken out respectively for float and sink analysis, and the partition curve was drawn, as shown in Figure 10. Compared with the ADMFB, the VDMFB can reduce the separation probable error from 0.134 to 0.083 g/cm^3 and the ash content of clean coal from 18.83 to 14.97%. The vibration energy significantly improves the separation effect of the ADMFB on fine coal.

https://doi.org/10.1021/acsomega.1c01034
ACS Omega 2021, 6, 14268−14277

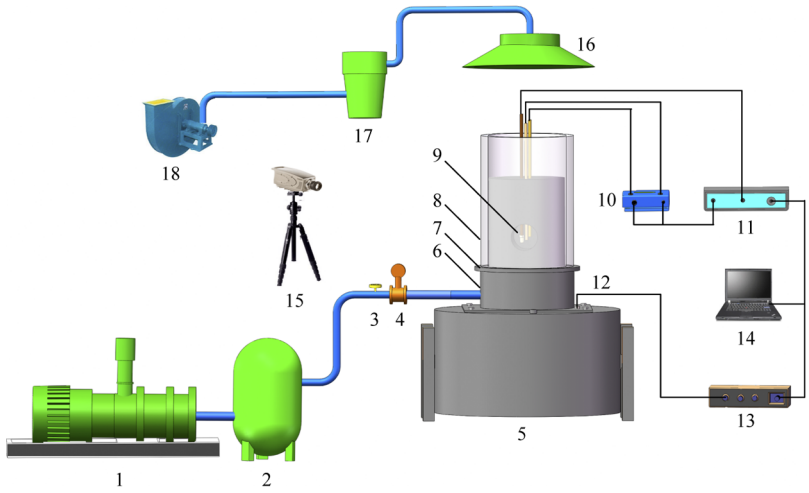

Figure 11. Schematic diagram of the VDMFB separation system. 1- blower; 2- buffer tank; 3- electromagnetic valve; 4- flowmeter; 5- electromagnetic vibrating table; 6- pre-gas distribution chamber; 7- gas distributor; 8- fluidization chamber; 9- force sensor; 10- pressure drop sensor; 11- data acquisition card; 12- acceleration sensor; 13- vibration controller; 14- computer; 15- high-speed dynamic camera; 16- dust absorbing cover; 17- dust filter; 18- air exhauster.

3. CONCLUSIONS

(1) R_{imp} can effectively evaluate the improvement effect of vibration energy on fluidization quality. When $I_{u,v} < I_{u,c}$, and $R_{imp} < 0$, it reflected that the vibration introduced at this time was not conducive to the stability of bed density. When $I_{u,v} > I_{u,c}$, and $R_{imp} > 0$, it showed that the vibration energy improved the fluidization quality. The higher the R_{imp} value was, the more obvious the improvement effect was. When $I_{u,v} = 1$ and $R_{imp} = 1$, it indicated that the density distribution of the VDMFB was completely uniform. When $I_{u,c} = 1$, it showed that the density distribution of the ordinary gas−solid fluidized bed was completely uniform, and the introduction of vibration was meaningless.

(2) VDMFB can be divided into three regions, that is, microbubble formation region ($H < 40$ mm), bubble merging inhibition region ($H = 40-150$ mm), and bubble fast merging and breaking region ($H > 150$ mm). In the region of $H < 40$ mm, the randomly generated microbubbles caused significant random disturbance to the periodic pressure fluctuation, and the micro-bubbles were broken by vibration energy with difficulty. In the region of $H = 40-150$ mm, the vibration energy can restrain the coalescence of bubbles and form a uniform and stable continuous bed suitable for the separation of fine coal. In the region of $H > 150$ mm, the restraint of vibration on the behavior of particles and bubbles was greatly weakened, and the fluidization was closer to that of the ordinary gas−solid fluidized bed.

(3) Compared with the ADMFB, the VDMFB has a more obvious separation effect on fine coal (1−6 mm). The probable error was reduced from 0.134 to 0.083 g/cm^3, and the ash content of clean coal was reduced from 18.83 to 14.97%.

4. EXPERIMENTAL SECTION

4.1. Experimental Apparatus and Materials. The VDMFB system is shown in Figure 11. According to different functions, the test system was mainly divided into four parts: air supply unit, fluidization and separation unit, data acquisition and processing unit, and dust removal unit. The air supply unit comprises the blower, buffer tank, and electromagnetic valve. The blower and buffer tank form a constant compressed air source to provide uniform and stable gas for fluidization. The electromagnetic valve adjusts the air velocity in real time within the range of 0−50 cm/s. The fluidization and separation unit mainly includes the electromagnetic vibration table and its control device, the pre-gas distribution chamber, gas distributor, and the fluidized bed. The vibration energy of the VDMFB comes from an electromagnetic vibrating table. The electromagnetic coil inside the electromagnetic vibrating table cyclically cuts the alternating magnetic field so that the vibrating table generates simple harmonic vibration in the vertical direction. The vibration controller is used to adjust the vertical simple harmonic vibration of the electromagnetic vibrating table. The electromagnetic vibrating table, pre-gas distribution chamber, gas distributor, and fluidization chamber are connected by bolts in sequence. The electromagnetic vibrating table transfers the vibration energy to the pre-gas distribution chamber, the gas distributor, and the side wall of the fluidization chamber in turn, so that they can perform synchronous vertical vibration. The particles are placed in the fluidization chamber and accumulated on the gas distributor. The air from the blower passes through the gas distributor and enters the fluidization chamber evenly. The vibrating gas distributor and the rising gas jointly drive the particles in the fluidization chamber to fluidize. The fluidization chamber is made of plexiglass, with the inner diameter of 200 mm and the height of 400 mm. The gas distributor is a stainless steel sintered porous plate with the thickness of 5 mm, and the average aperture of the porous plate is 5 μm.

A certain amount of 0.1−0.3 mm magnetite powder was placed in the fluidization chamber, and the height of the static bed is 200 mm. The main physical properties of the magnetite powder is shown in Table 2. After air flow and vibration were applied, the magnetite powder was fluidized by the combination of upward gas flow and vibration. The pressure drop sensor, acceleration sensor, data acquisition card, and computer together constitute the data acquisition and processing unit, which can collect and analyze the bed pressure and vibration signals in the process of bed fluidization in real time. The

https://doi.org/10.1021/acsomega.1c01034
ACS Omega 2021, 6, 14268−14277

Table 2. Main Physical Properties of Magnetite Powder

size/mm	yield/%	true density/g/cm^3	bulk density/g/cm^3
0.1−0.2	37.26	4493	2669
0.2−0.3	62.74	4603	2577
0.1−0.3	100	4560	2612

induced draft hood, dust collector, and induced draft fan constitute the dust removal unit, which cooperates with the exhauster head and tail to guide the directional flow of air flow, timely collect the air mixed with dust generated in the test process, and purify the dust, so as to ensure the cleanness of the test environment and the recovery of test materials.

During the separation, 6−1 mm raw coal is fed into the fluidized bed from the upper part of the bed layer, and the air flow and vibration are cut off after 20 s. The coal samples are taken out layer by layer from the top to the bottom for weighing and testing. The density and ash distribution of 6−1 mm raw coal is shown in Figure 12.

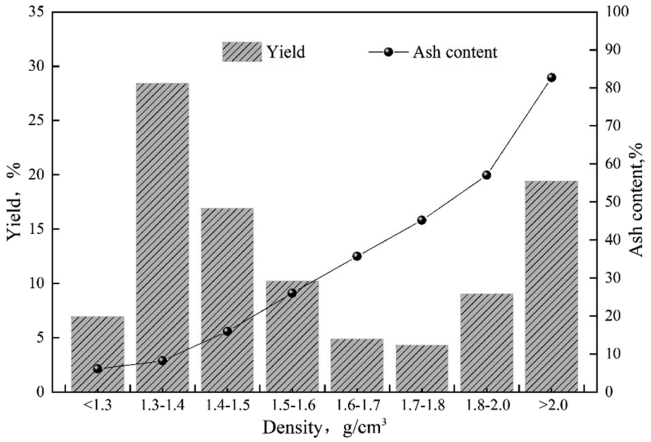

Figure 12. Density and ash distribution of 6−1 mm raw coal.

4.2. Data Processing. *4.2.1. Evaluation Method of the Fluidized Bed Quality, σ_ρ and SK$_\rho$.* The fluidization quality of the VDMFB for coal separation is mainly evaluated by the uniform stability of bed density distribution. The density standard deviation σ_ρ is used to reflect the uniformity of bed density distribution in the measurement area. The skewness of bed density at different measurement areas, SK$_\rho$, which is used to evaluate the deviation trend of density measurements compared to the average density.[20]

$$\sigma_\rho = \sqrt{\frac{1}{n}\sum_{i=1}^{n}(\rho_i - \rho_a)^2} \quad (1)$$

$$SK_\rho = \frac{n\sum_{i=1}^{n}(\rho_i - \rho_a)^3}{(n-1)(n-2)\sigma_\rho^3} \quad (2)$$

where n is the number of measurement points, ρ_i is the bed density measurement value at the ith test point, g/cm^3, and ρ_a is the average value of n bed density measurements, g/cm^3.

4.2.2. Evaluation Method for Improving the Fluidization Quality by Vibration, R_{imp}. In the bubbling fluidization stage of the VDMFB, the bed consists of two parts: bubble phase and emulsion phase. The volumes of the bubble phase and emulsion phase are V_b and V_e, respectively, and the densities are ρ_b and ρ_e, respectively. In the paper,[21] the author pointed out that if the volume fraction of emulsion is m, then $m = V_e/(V_e + V_b)$. Assuming that all bubbles in the fluidized bed converge into a large bubble, the variance of density distribution in the fluidized bed is as follows

$$\sigma_\rho^2 = m(\rho_e - \bar{\rho})^2 + (1-m)(\rho_b - \bar{\rho})^2 = (\rho_e - \rho_b)^2(m - m^2) \quad (3)$$

There are few bubbles in the critical fluidization state of the VDMFB, so m is approximately equal to 1. With the increase of gas velocity, the suppression effect of vibration on bubbles is weakened. When the fluctuation range of bed density is close to that of the nonvibrated fluidized bed, the effect of vibration on improving bed density uniformity almost disappears. Previous studies show that the maximum expansion rate of the bed is about 25% in the bubbling stage.[22,23] Since the volume of emulsion phase is constant, m = 0.8. Therefore, for the VDMFB, the value of m is 0.8−1. The derivation of eq 2 shows that

$$\frac{d\sigma_\rho^2}{dm} = (\rho_e - \rho_b)^2(1-2m) \quad (4)$$

$\rho_b \ll \rho_e$, when m = 0.8−1, $d(\sigma_\rho^2)/dm < 0$, indicating that when m = 0.8, σ_ρ^2 reaches the maximum and the bed density uniformity is the lowest. The bed density variance σ_ρ^2 under different operating gas velocities is calculated and compared with the maximum variance of bed density when m = 0.8. It is defined as the bed density uniformity index

$$I_u = (\sigma_{\rho(m=0.8)}^2 - \sigma_\rho^2)/\sigma_{\rho(m=0.8)}^2 \quad (5)$$

The value of I_u is in the range of 0−1. The higher the value is, the higher the density uniformity is. When I_u = 1, the bed density is completely uniform. Comparing the bed density uniformity index of vibrated fluidized bed with that of the non-vibrated fluidized bed under the same gas velocity, the following results can be obtained

$$R_{imp} = \begin{cases} I_{u,v} & U_{mfv} \le U \le U_{mfc} \\ \dfrac{I_{u,v} - I_{u,c}}{1 - I_{u,c}} & U > U_{mfc} \end{cases} \quad (6)$$

$I_{u,v}$ and $I_{u,c}$ are the bed density uniformity index of the vibrated fluidized bed and non-vibrated fluidized bed, respectively. R_{imp} indicates the improvement effect of vibration on fluidization quality. The higher the value is, the more obvious the improvement effect is.

AUTHOR INFORMATION

Corresponding Author

Enhui Zhou − *School of Chemical Engineering & Technology, China University of Mining & Technology, Xuzhou 221116, China*; orcid.org/0000-0002-8936-2387; Email: zeh@cumt.edu.cn

Authors

Yadong Shan − *School of Chemical Engineering & Technology, China University of Mining & Technology, Xuzhou 221116, China*

Linhai Li − *Shenhua Xinjiang Energy Co., Ltd., Toksun 838100, China*

Fanshun Shen − *Shenhua Xinjiang Energy Co., Ltd., Toksun 838100, China*

https://doi.org/10.1021/acsomega.1c01034
ACS Omega 2021, 6, 14268−14277

Enkhsaruul Byambajav − *Department of Chemistry, School of Arts & Sciences, National University of Mongolia, Ulaanbaatar 210646, Mongolia*
Bo Zhang − *School of Chemical Engineering & Technology, China University of Mining & Technology, Xuzhou 221116, China;* orcid.org/0000-0001-7963-4572
Changxing Shi − *School of Chemistry and Environmental Engineering, North China Institute of Science & Technology, Sanhe 065201, China*

Complete contact information is available at: https://pubs.acs.org/10.1021/acsomega.1c01034

Notes

The authors declare no competing financial interest.

■ ACKNOWLEDGMENTS

This work was supported by the Fundamental Research Funds for the Central Universities (no. 2019QNA06).

■ REFERENCES

(1) British Petroleum. *BP Statistical Review of World Energy 2020*, 2020.
(2) Moshood, O.; Bekir, G.; Samson, B. Spontaneous combustion liability between coal seams: A thermogravimetric study. *Int. J. Min. Sci. Technol.* **2020**, *30*, 691−698.
(3) Boylu, F.; Talı, E.; Çetinel, T.; Çelik, M. S. Effect of fluidizing characteristics on upgrading of lignitic coals in gravity based air jig. *Int. J. Miner. Process.* **2014**, *129*, 27−35.
(4) Chalavadi, G.; Das, A. Study of the mechanism of fine coal beneficiation in air table. *Fuel* **2015**, *154*, 207−216.
(5) Chalavadi, G.; Singh, R. K.; Sharma, M.; Singh, R.; Das, A. Development of a generalized strategy for dry beneficiation of fine coal over a vibrating inclined deck. *Int. J. Coal Prep. Util.* **2015**, *36*, 10−27.
(6) Zhang, B.; Akbari, H.; Yang, F.; Mohanty, M. K.; Hirschi, J. Performance optimization of the FGX dry separator for cleaning high-sulfur coal. *Int. J. Coal Prep. Util.* **2011**, *31*, 161−186.
(7) Zhao, Y.; Yang, X.; Luo, Z.; Duan, C.; Song, S. Progress in developments of dry coal beneficiation. *Int. J. Coal Sci. Technol.* **2014**, *1*, 103−112.
(8) Yang, X.; Zhao, Y.; Luo, Z.; Song, S.; Chen, Z. Fine coal dry beneficiation using autogenous medium in a vibrated fluidized bed. *Int. J. Miner. Process.* **2013**, *125*, 86−91.
(9) Dwari, R. K.; Rao, K. H. Dry Beneficiation of Coal-a Review. *Miner. Process. Extr. Metall. Rev.* **2007**, *28*, 177−234.
(10) Luo, Z.; Fan, M.; Zhao, Y.; Tao, X.; Chen, Q.; Chen, Z. Density-dependent separation of dry fine coal in a vibrated fluidized bed. *Powder Technol.* **2008**, *187*, 119−123.
(11) Morse, R. D. Sonic energy in granular solid fluidization. *Ind. Eng. Chem.* **1955**, *47*, 1170−1175.
(12) Mujumdar, A. Aerodynamics, heat transfer and drying in vibrated fluid beds. *Am. J. Heat Mass Transfer* **1983**, *7*, 99−110.
(13) Bratu, E.; Jinescu, G. Heat-transfer in vibrated fluidized layers. *Rev. Roum. Chim.* **1972**, *17*, 49−56.
(14) Gutman, R. Vibrated beds of powders part 1: a theoretical model for the vibrated bed. *Instn. Chem. Engrs.* **1976**, *54*, 174−183.
(15) Jin, H. *Fluidization characteristics and particle separation in vibrated fluidized beds*; Taiyuan, Institute of Coal Chemistry, Chinese Academy of Sciences, 1998.
(16) Tanaka, Z.; Song, X. Continuous separation of particles by fluidized beds. *Adv. Powder Technol.* **1996**, *7*, 29−40.
(17) Di Maio, F. P.; Di Alberto, R.; Vincenzino, V. Extension and validation of the particle segregation model for bubbling gas-fluidized beds of binary mixtures. *Chem. Eng. Sci.* **2013**, *97*, 139−151.
(18) Lv, B. *Diffusion and Separation Mechanism of Multi-Component Materials in Gas−Solid Separation Fluidized Bed*; China University of Mining &Technology: Xuzhou, 2019.
(19) Zhou, E.; Zhang, Y.; Zhao, Y.; Luo, Z.; He, J.; Duan, C. Characteristic gas velocity and fluidization quality evaluation of vibrated dense medium fluidized bed for fine coal separation. *Adv. Powder Technol.* **2018**, *29*, 985−995.
(20) Luo, Z.; Zhao, Y. *Separation Theory of Fluidization*, 1st ed.; China University of Mining and Technology Press: Xuzhou, 2002.
(21) Jin, Y.; Zhu, J.; Wang, Z.; Yu, Z. *Fluidization engineering Principles*, 1st ed.; Tsinghua University Press: Beijing, 2001.
(22) Zhou, E.; Zhang, Y.; Zhao, Y.; Luo, Z.; Duan, C.; Yang, X.; Dong, L.; Zhang, B. Collaborative optimization of vibration and gas flow on fluidization quality and fine coal segregation in a vibrated dense medium fluidized bed. *Powder Technol.* **2017**, *322*, 497−509.
(23) Gao, Z.; Chai, X.; Zhou, E.; Jia, Y.; Duan, C.; Tang, L. Effect of the distributor plugging ways on fluidization quality and particle stratification in air dense medium fluidized bed. *Int. J. Min. Sci. Technol.* **2020**, *30*, 883−888.